MAGNETIC SUSCEPTIBILITY OF POWDERED $SmPO_4$

MAGNETIC SUSCEPTIBILITY OF POWDERED $SmPO_4$

by

Ronald J.J. Cannata, B.Sc.

A Thesis

Submitted to the Faculty of Graduate Studies

in Partial Fulfilment of the Requirements

for the Degree

Master of Science

McMaster University

March 1971

MASTER OF SCIENCE
(Physics)

McMASTER UNIVERSITY
Hamilton, Ontario

TITLE: Magnetic Susceptibility of Powdered $SmPO_4$

AUTHOR: Ronald J.J. Cannata, B.Sc. (York University)

SUPERVISOR: Dr. C.V. Stager

NUMBER OF PAGES: vi, 39

SCOPE AND CONTENTS:

The magnetic susceptibility of samarium orthophosphate ($SmPO_4$) has been measured over the temperature range from 0.4 to 270°K. A theoretical expression for the susceptibility has been developed assuming a crystal field of cubic symmetry and fitted to the experimental data.

ACKNOWLEDGEMENTS

I would like to thank my supervisor, Dr. C.V. Stager, for his patience, understanding and guidance during the past year.

I am grateful to Colin Fowlis and Ralph Kuehnel for their many enlightening discussions and to all those who provoked and expanded my thoughts.

I wish to dedicate this work to my parents and to Karen.

TABLE OF CONTENTS

LIST OF ILLUSTRATIONS

LIST OF TABLES

CHAPTER I

INTRODUCTION

The rare earth phosphates, arsenates and vanadates form two series of isomorphous compounds. They crystallize with either a monoclinic or a tetragonal crystal structure (Schwarz, 1963). Single crystals are relatively easy to grow by a flux method (Feigelson, 1964). For the above reasons these series should be promising candidates for an investigation of the problem of a magnetic impurity in an ordered magnetic structure by microwave techniques. There is, however, very little information available about the magnetic properties of these systems. To initiate a systematic study, we have measured the magnetic susceptibility of monoclinic $SmPO_4$ above 4.2°K using a vibrating sample magnetometer. In addition, we have built an apparatus to measure the a.c. susceptibility over the temperature range 0.4 to 4.2°K.

An expression has been developed for the susceptibility of the Sm^{3+} ion that includes the effects of spin-orbit coupling and the cubic crystal field splitting of the ground state. The parameters which describe these effects have been determined by fitting the expression to the experimental results.

The remainder of the introduction presents a description of the Sm^{3+} ion. In Chapter II we give the theory necessary for interpreting the data. A complete description of the

apparatus and the theory of the most important components is presented in Chapter III. Chapter IV describes the method used to obtain low and high temperature data. The analysis and experimental results are given in Chapter V, followed by a discussion of the results and conclusions in Chapter VI.

The lowest energy electron configuration for Sm^{3+} is $4f^5 5s^2 5p^6$. The 4f shell is partially filled with electrons and is somewhat shielded from external electric field effects by the $5s^2 5p^6$ electrons. The effect of electron-electron interactions is to produce a ^6H ground state and the spin-orbit interaction splits this state into six multiplets of definite J. Each multiplet is (2J+1)-fold degenerate. In this approximation the states may be labelled by $|\alpha LSJM\rangle$. The J=5/2 state lies lowest in energy. In a cubic crystal field a J=5/2 state splits into a 2 and a 4-fold degenerate state labelled by Γ_7 and Γ_8 while the next lowest state J=7/2 splits into two 2 and one 4-fold degenerate states Γ_6', Γ_7', Γ_8'. The Γ_i are labels for the irreducible representations of the cubic group (Griffith, 1964). An illustration of the splittings of a ^6H term under spin-orbit, cubic crystal field and magnetic field interactions is shown in Fig. 1. We assume that the Γ_7 state lies lowest in energy.

Dieke (1968) indicates that the $^6H_{5/2} - {}^6H_{7/2}$ splitting, Δ, is $\sim$1100 cm^{-1} and that the overall crystal field splitting, K, is $\sim$70 cm^{-1} for Sm^{3+} in hexagonal $LaCl_3$. The spin-orbit splitting in $SmPO_4$ would not be expected to

Figure 1

The lowest energy levels of the ^6H term of Sm^{3+}

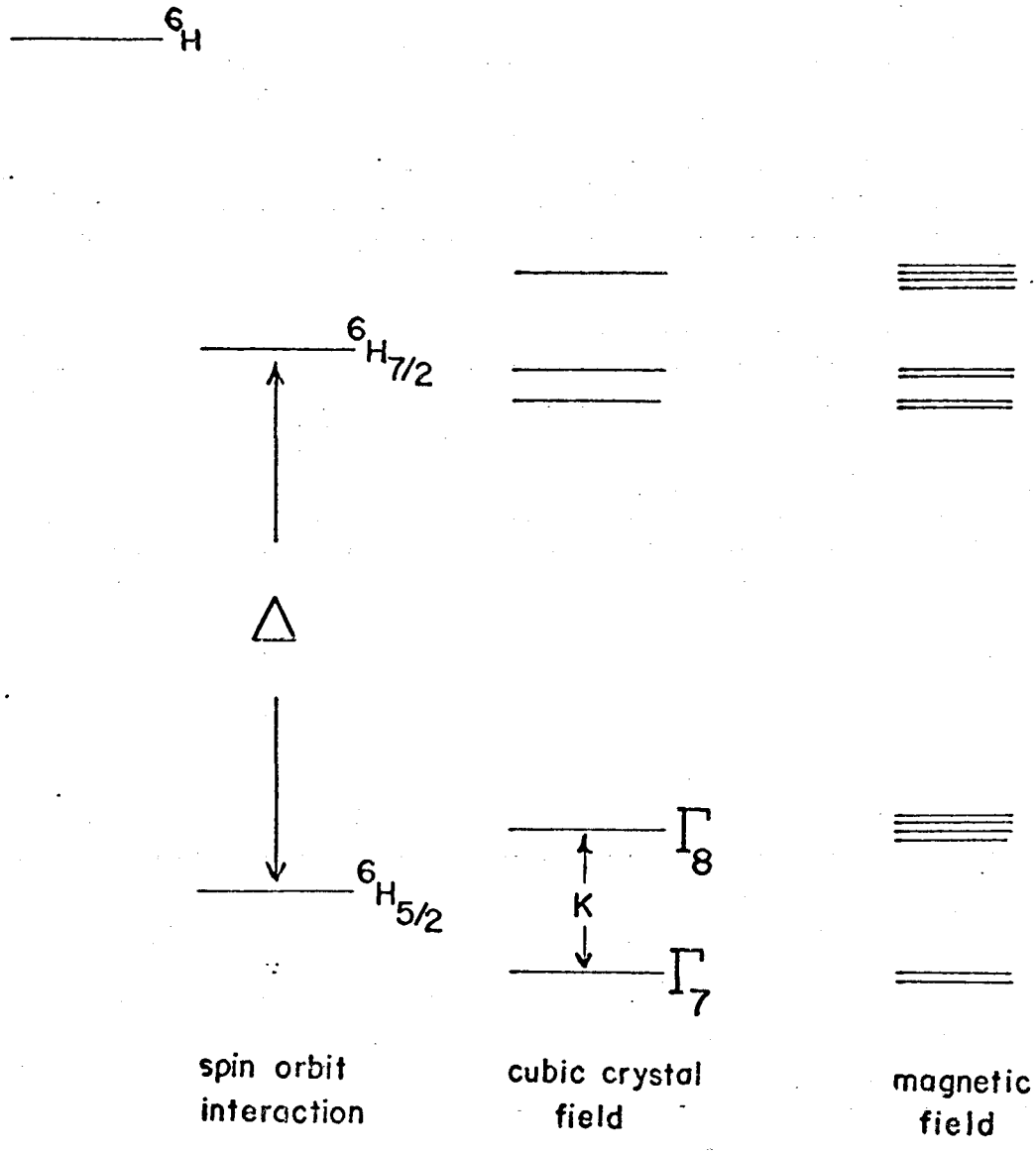
^6H
$^6H_{7/2}$
Δ
$^6H_{5/2}$
Γ_8
K
Γ_7
spin orbit interaction
cubic crystal field
magnetic field

Figure 1

differ by more than 10% from the above value since any crystal effects on the energy levels are much smaller than spin-orbit effects. The crystal field splitting could be appreciably different since $SmPO_4$ does not have a hexagonal crystal structure and the crystal field is not cubic.

CHAPTER II

THEORY

THE CRYSTAL FIELD

In this section we introduce the effect of a static cubic crystal field on the free Sm^{3+} ion. The interaction Hamiltonian will be developed and a method for calculating crystal field matrix elements will be presented.

The exchange interaction between samarium ions is very weak since no magnetic ordering occurs; therefore, one makes the approximation that the ion is isolated and perturbed only by a static electric field produced by neighbouring anions. This effect is small ($<100\ cm^{-1}$) compared to the spin-orbit interaction and hence may be treated by perturbation theory.

One can expand the static crystal field about an ion as a series in spherical harmonics. In the cubic field case, for f electrons, the interaction may be written (Low 1960)

$$V = A_4^o \left(Y_4^o + \sqrt{\frac{5}{14}} \left(Y_4^4 + Y_4^{-4}\right)\right)$$

$$+ A_6^o \left(Y_6^o + \frac{\sqrt{14}}{2} \left(Y_6^4 + Y_6^{-4}\right)\right)$$

where the general spherical harmonic is Y_k^q and the A_k^q's are crystal field parameters.

The fact that terms in $q \neq 0$ exist may cause a mixing of free ion eigenstates with different M values. M would no longer be a good quantum number to label the states with.

We use the Wigner-Eckart theorem to find the matrix elements of any tensor operator T_k^q with respect to free ion states characterized by $|LSJM\rangle$.

Once one has determined the interaction matrix, it must be diagonalized to find the eigenvalues and eigenvectors. The crystal field is much smaller than the spin-orbit energy so that it can be treated by first order perturbation theory. In first order there is no mixing of states with different values of J. Since the J=7/2 state is $\sim$1100 cm^{-1} above the ground state it will never be substantially populated so that it is only necessary to consider the effect of the crystal field on the J=5/2 level for the susceptibility below room temperature.

MAGNETIC SUSCEPTIBILITY

In this section we will outline the procedure for obtaining the magnetic susceptibility and VanVleck's (1932) formula for the susceptibility.

The magnetic moment μ of an ion in its n^{th} level in an applied magnetic field H in the z direction is given by

$$\mu_n = - \partial E_n / \partial H.$$

E_n is the energy of the level in which the dipole exists. The energy of the n^{th} level may be expanded in a series in matrix elements of the perturbing Hamiltonian,

$$H' = \mu_z H = \mu_o (L_z + 2S_z) H.$$

According to standard perturbation theory:

$$E_n = E_n^o + H\, E_{nm}^{(1)} + H^2\, E_{nm}^{(2)} + \ldots$$

where $$E_{nm}^{(1)} = \langle \psi_{nm} | \mu_z | \psi_{nm} \rangle$$

$$E_{nm}^{(2)} = \sum_{n',m'} \frac{|\langle \psi_{nm} | \mu_z | \psi_{n'm'} \rangle|^2}{E_n - E_{n'}}$$

There is a thermal distribution of aligned dipoles in the various energy levels in the presence of a magnetic field. The total magnetic susceptibility χ is a statistical mean over all stationary states using a Boltzmann distribution,

$$\chi = \frac{N \sum_{n,m} \mu_{nm}\, e^{-E_n/kT}}{H \sum_{n,m} e^{-E_n/kT}}$$

where N is the number of atoms per mole. The above expression for the susceptibility is exact.

It can be shown that if the argument of the exponential is written as the series expansion for E_n and the exponential is then expanded for small arguments, that the susceptibility becomes:

$$\chi = \frac{N \sum_{nm} \left[\frac{(E_{nm}^{(1)})^2}{kT} - 2\, E_{nm}^{(2)} \right] e^{-E_n^o/kT}}{\sum_{nm} e^{-E_n^o/kT}}$$

The term in $E_{nm}^{(1)}$ is the Curie type contribution to the susceptibility and the term in $E_{nm}^{(2)}$ is the temperature independent VanVleck susceptibility arising from the magnetic interaction between states of different energies.

THE SUSCEPTIBILITY EXPRESSION

The effect of the crystal electric field and a magnetic field along the z direction on the $^6H_{5/2}$ level of the Sm^{3+} ion may be treated exactly. Corrections to the susceptibility due to the presence of the J=7/2 state are included by using second order perturbation theory.

Since the magnetic field is along the z axis, matrix elements in $L_z + 2S_z$ are required. If R_x, R_y and R_z are the components of a vector operator then from the theory of irreducible tensor operators one defines $R_z=R_1^o$; that is, R_z is the zeroth component of an irreducible tensor of order 1. The Wigner-Eckart theorem may be employed to calculate the matrix elements.

For the free ion one finds that for J=5/2

$$\langle JM|L_z + 2S_z|JM'\rangle = -\frac{2}{7} M \delta_{MM'}.$$

The factor 2/7 is the Landé g factor for the free samarium ion. Thus writing the perturbation Hamiltonian as

$$H' = V + \mu_z H$$

and calculating the matrix elements one sees that the magnetic field adds terms only along the diagonal of the matrix of V. The matrix can be diagonalized to find the eigenvectors and eigenvalues. These eigenvalues may be used to calculate μ_{nm} from which the susceptibility may be obtained.

To complete the expression for the susceptibility we must include the contribution of the VanVleck term between the J=5/2 and J=7/2 states.

The contribution to the susceptibility from the J=5/2 state contains one adjustable parameters, the Γ_7-Γ_8 splitting, K, while the VanVleck term contains the other parameter, the $^6H_{5/2}$ - $^6H_{7/2}$ splitting, Δ. The energy separations are shown in Fig. 1.

The total susceptibility expression in units of emu/mole is

$$\chi = \frac{N\sum_{nm} \mu_{nm} e^{-E_n/kT}}{H\sum_{nm} e^{-E_n/kT}} - \frac{2Ne^{-E_n^o/kT}}{\sum_{nm} e^{-E_n^o/kT}} \left(\sum_{n'm'} |\langle \psi_{nm} | \mu_z | \psi_{n'm'} \rangle|^2 \right)$$

where n' = Γ_6', Γ_7', Γ_8'. $E_n - E_{n'}$ is assumed to be constant for all n'.

The eigenfunctions ψ_{nm} are tabulated by Griffith (1964). They are the perturbed wavefunctions due to a cubic crystal field and consist of linear combinations of the free ion states, |LSJM>.

CHAPTER III

EXPERIMENTAL APPARATUS

LOW TEMPERATURE APPARATUS

Diagrams of the apparatus used in measuring the magnetic susceptibility of $SmPO_4$ for temperatures below 4.2°K are shown in Figs. 2 and 3.

The primary coil was wound with 800 turns of #36 copper wire about a "micarta" coil form. Each layer was glued down with G.E. #7031 adhesive. The secondary was wound in two sections, a compensating and a measuring coil. These were connected in series opposition such that the mutual inductance between the primary and secondary was a minimum. Each side of the secondary had 2340 turns of #38 wire. Constantan wire provided the electrical path from the coils at 4.2°K to room temperature surroundings. The mutual inductance coils were immersed directly into the ^4He bath and surrounded the tip of the ^3He dewar.

Glass dewars were used as opposed to stainless steel ones because the latter can cause undesirable electromagnetic effects in the measuring equipment through the agency of eddy currents. There was provision on the ^3He dewar to admit ^4He "exchange gas" to the vacuum jacket to provide thermal equilibrium across the walls of that dewar. Thermal contact between the ^3He dewar inner-wall and the sample was maintained between 4.2°K and 1.2°K by means of ^3He gas.

Figure 2

Schematic illustration of the apparatus used in measuring a.c. susceptibility at ^{3}He temperatures.

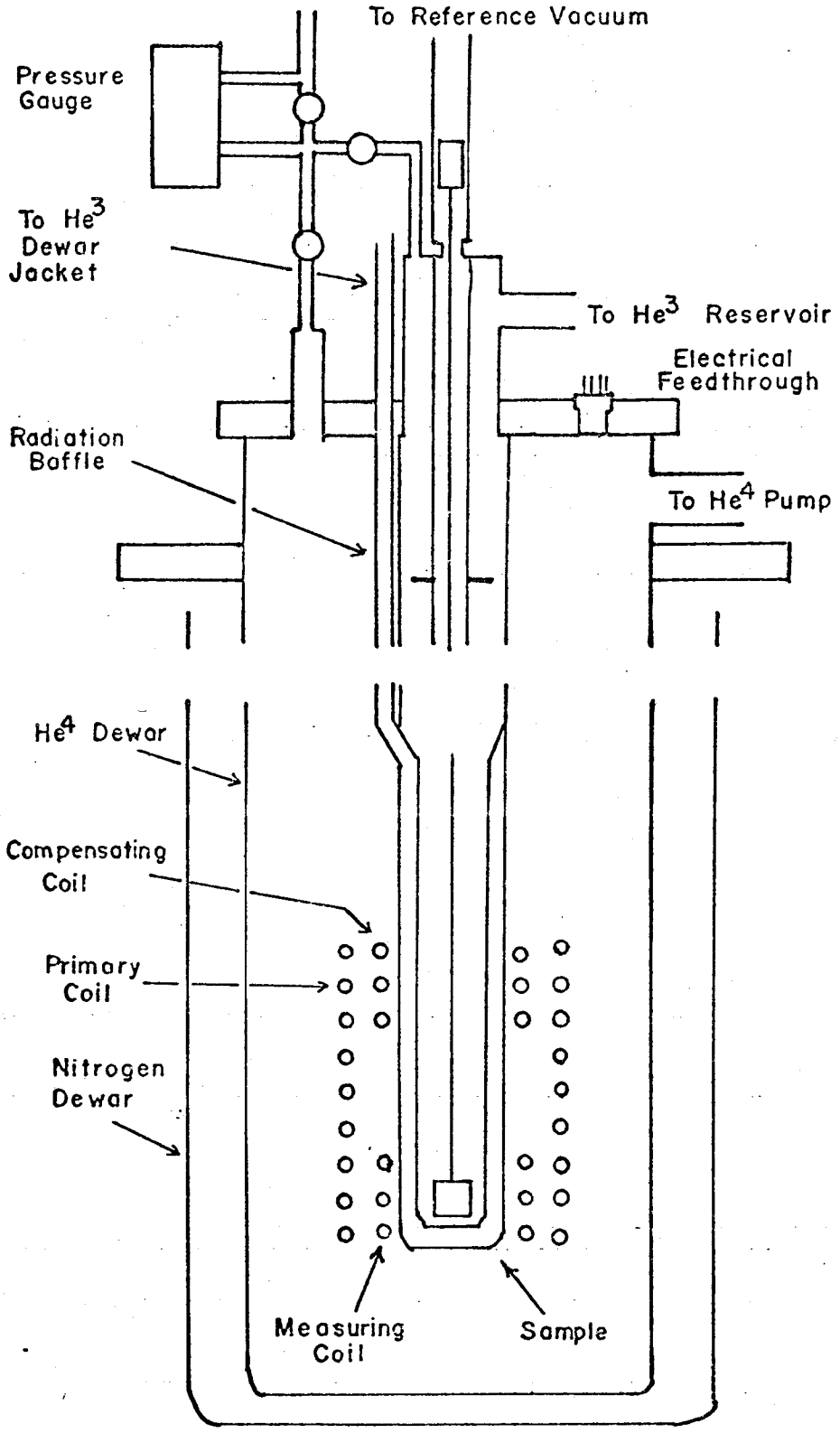
To Reference Vacuum
Pressure Gauge
To He^3 Dewar Jacket
To He^3 Reservoir
Electrical Feedthrough
Radiation Baffle
To He^4 Pump
He^4 Dewar
Compensating Coil
Primary Coil
Nitrogen Dewar
Measuring Coil
Sample

Figure 2

Figure 3

^{3}He gas handling system and pumping arrangement.

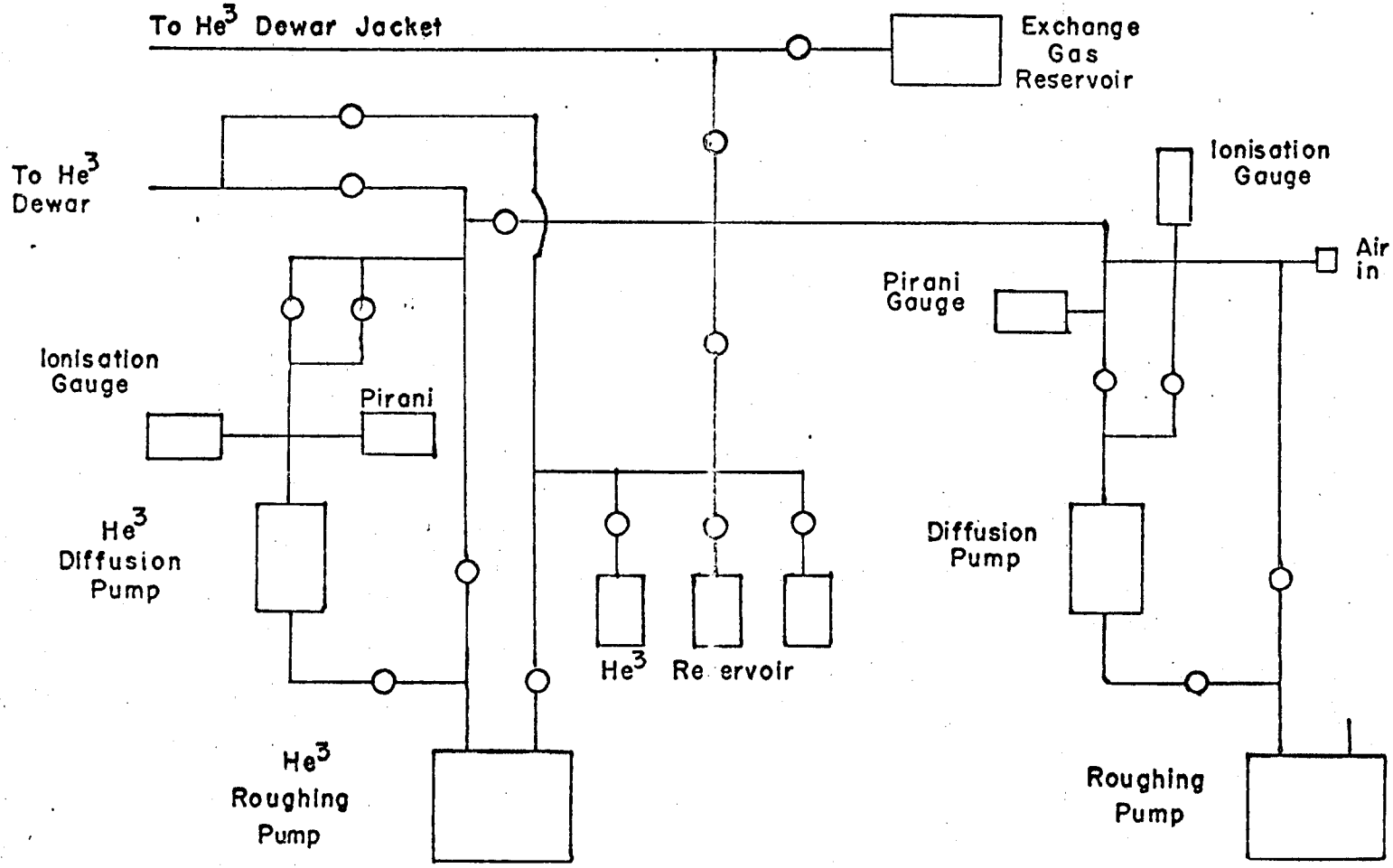
To He3 Dewar Jacket
Exchange Gas Reservoir
To He3 Dewar
Ionisation Gauge
Air in
Pirani Gauge
Ionisation Gauge
Pirani
He3 Diffusion Pump
Diffusion Pump
He3 Reservoir
He3 Roughing Pump
Roughing Pump

Figure 3

Temperature measurements in the range 4.2-1.2°K were obtained from the measured vapour pressure of ^{4}He using a Texas Instrument Precision Pressure Gauge, model 145. Valves were arranged so that this same instrument could be used to measure the ^{3}He vapour pressure. There was one pumping system to evacuate the ^{3}He dewar initially and the dewar jacket, and a separate system to return the ^{3}He to storage reservoirs.

Fig. 2 shows how a permanent magnet, external to the ^{3}He vacuum system, could be used to lift the sample out of the measuring coils. This operation permitted an accurate determination of the background signal due to an unbalance in the coils.

Three baffles were soldered to a stainless steel rod to reflect any radiation from the warmer parts of the ^{3}He dewar. A piece of paper was coated with powdered graphite and inserted between the coil and the ^{3}He dewar to minimize the room temperature radiation that could penetrate into the section of the ^{3}He dewar containing the liquid.

The coupling, that is, the mutual inductance between the primary and the pair of series opposed secondaries has two contributions. One is due to the sample and the other is due to the background in the absence of the sample. The difference in these contributions at a given temperature is proportional to the susceptibility (and weight) of the sample at that temperature. These mutual inductance measurements were made with a Cryotronics mutual inductance bridge

model ML-155B. Measurements involve balancing the induced emf in the secondary of the mutual inductance containing the sample by means of a variable mutual inductance connected in series opposition. The bridge was similar to that described by Pillinger et al. (1958). A simplified representation of the circuit is shown in Fig. 4. A signal generator is transformer coupled with the primary circuit and gives rise to a primary current which passes through a decade resistor, ρ. This resistor and the triode tube form an artificial primary circuit feeding the fixed mutual inductor, m. Adjusting ρ changes the current in the artificial circuit and hence the induced voltage in the secondary of m. Out of phase components in the secondary are balanced by varying R. An oscilloscope provides visual observation of the null balance.

HIGH TEMPERATURE APPARATUS

Susceptibility measurements above 4.2°K were performed using a Princeton Applied Research vibrating sample magnetometer model FM-1, in conjunction with a magnion model L-96 magnet. An illustration is shown in Fig. 5.

The sample is vibrated along a line pendicular to the applied magnetic field. The resulting oscillating dipolar field is detected by a pair of pick-up coils. The magnitude of the signal induced in the coils is proportional to the magnetic moment of the sample and to the vibration

Figure 4

Simplified representation of the a.c. mutual inductance bridge circuit.

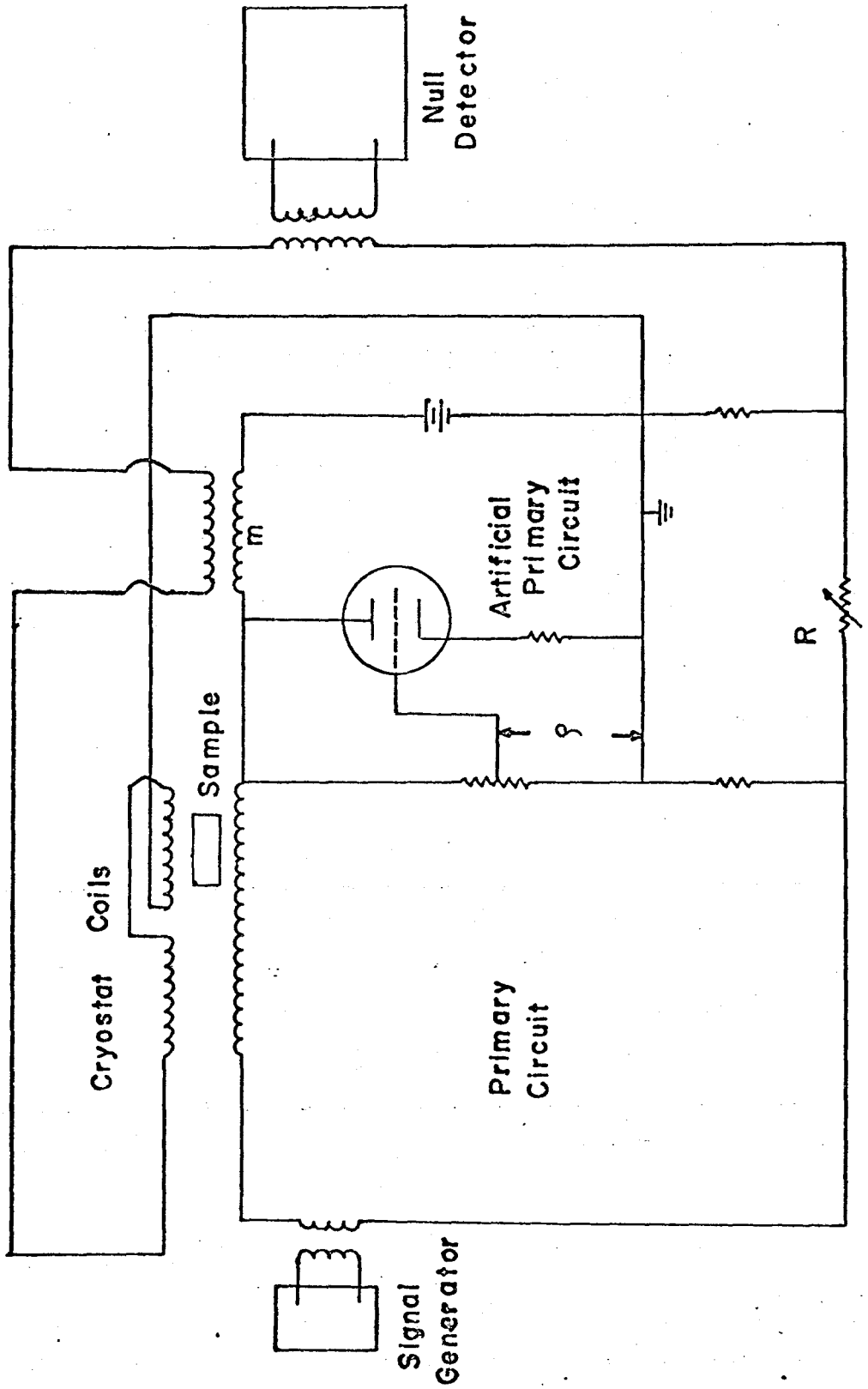
Null Detector
m
Artificial Primary Circuit
R
Sample
Cryostat Coils
Primary Circuit
Signal Generator

Figure 4

Figure 5

Schematic illustration of the vibrating sample magnetometer.

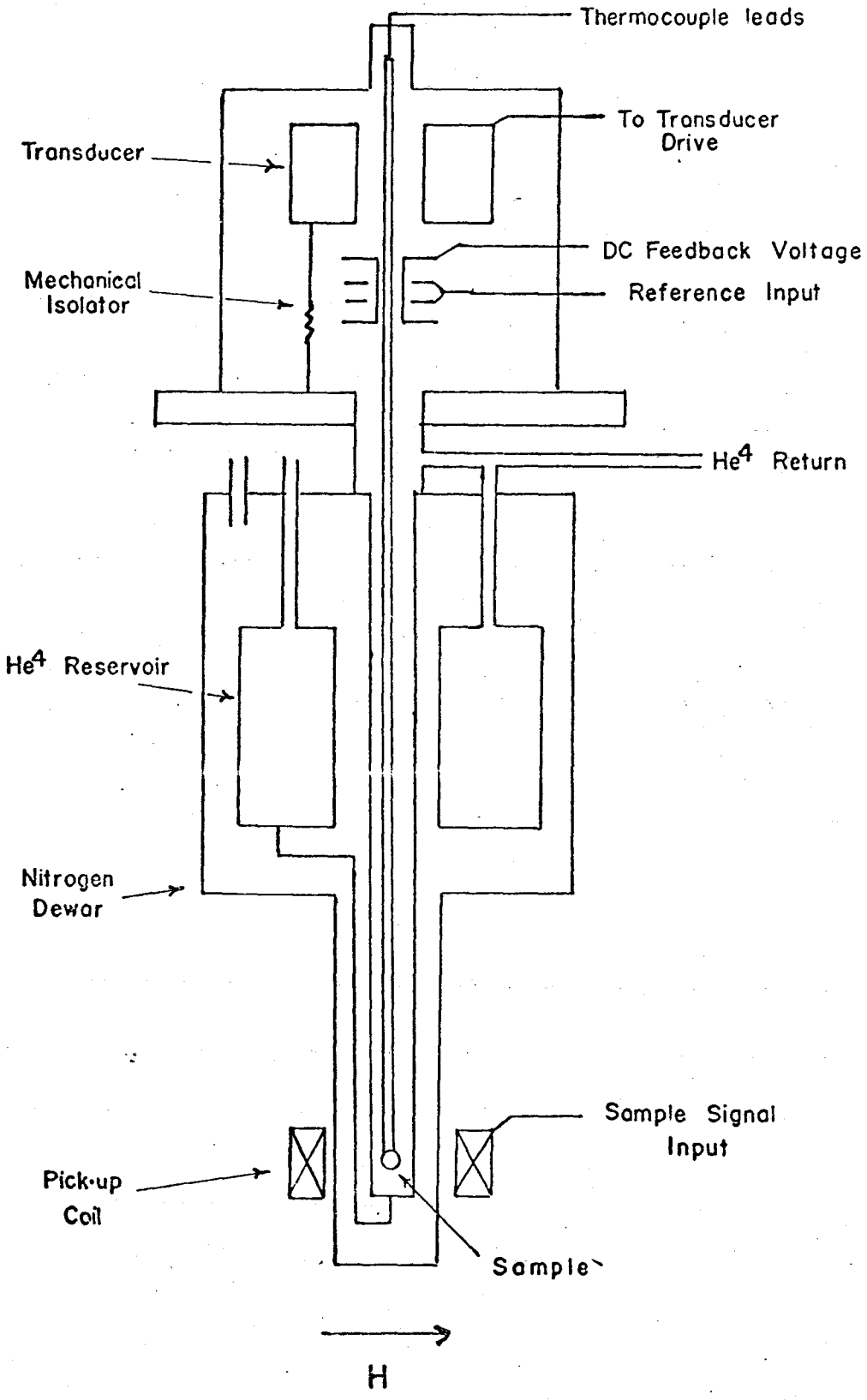
Thermocouple leads
To Transducer Drive
Transducer
DC Feedback Voltage
Mechanical Isolator
Reference Input
He4 Return
He4 Reservoir
Nitrogen Dewar
Sample Signal Input
Pick-up Coil
Sample
H

Figure 5.

frequency and amplitude. At the same time a pair of capacitor plates bearing a DC voltage vibrate at the same frequency between a pair of fixed capacitor plates. This induces a reference signal on the fixed plates. The sample signal is compared to the reference signal and the difference is converted to a DC voltage and fed back to the vibrating capacitor plates to obtain a null between the reference and sample signals. This nulling technique insures that the measured result is independent of the vibration frequency and amplitude. The DC feedback voltage on the capacitor plates is proportional to the magnetic moment of the sample. A fraction of this voltage appears across the output terminals of the magnetometer.

CHAPTER IV

EXPERIMENTAL METHOD

PREPARATION OF THE SAMPLE

The flux method (Feigelson 1964) was used to grow $SmPO_4$ crystals. A few grams of lead pyrophosphate ($Pb_2P_2O_7$) were placed at the bottom of a platinum crucible. Samarium oxide (Sm_2O_3) was added and the crucible was filled with $Pb_2P_2O_7$ and covered tightly. The ratio of $Pb_2P_2O_7$:Sm_2O_3 was 24:1 by weight.

The crucible was heated to 1300°C at a rate of 300°C/hour and allowed to soak for 12 hours to assure complete dissolution of the oxide and then cooled to 950°C at a rate of 3°C/hour. The solidified matrix of $Pb_2P_2O_7$ in which the $SmPO_4$ crystals were imbedded was removed by leaching with hot dilute nitric acid.

LOW TEMPERATURE MEASUREMENTS

To measure the a.c. susceptibility below 4.2°K a 0.315 gram sample was used. Liquid nitrogen and helium were transferred into their respective dewars. ^4He exchange gas was admitted to the ^3He dewar jacket and ^3He gas was admitted to the sample chamber. The liquid helium was pumped slowly down to 1.2°K while the bridge was balanced at intervals of 0.05°K. When the ^3He gas had liquified, the exchange gas was pumped away. Further measurements were

made while the pressure over the ^3He was slowly reduced by pumping. At frequent intervals the sample was removed from the coils to obtain a background reading.

The conversion factor from units of mutual inductance to units of susceptibility was determined using a known weight of Cerium Magnesium Nitrate (CMN) whose susceptibility is known to be (Schriempe et al., 1964)

$$\chi = (0.213 + \frac{2.73}{T})10^{-4} \text{ emu/gm.}$$

HIGH TEMPERATURE MEASUREMENTS

The procedure for obtaining high temperature susceptibility measurements was as follows. A 0.924 gram powdered sample of $SmPO_4$ was cooled in the sample position shown in Fig. 5. Liquid helium was allowed to flow into the sample chamber from below. A heater beneath the sample created a continuous stream of helium gas whose temperature was continuously controlled over the range from 4.2°K to room temperature. A thermocouple of chromel versus gold-0.02 atomic percent iron was used to measure the temperature. The thermocouple was located at the center of the sample and referenced to an ice-water bath.

Data was recorded, at suitable intervals in time, using a digital data acquisition system consisting of an X-1 and X-2 digital voltmeter and a serial converter which controlled the punching of data on paper tape.

Experimental runs were done with the sample present and with the sample absent so that background effects could be cancelled. The magnetometer was calibrated using a 1.10 gram nickel sample whose magnetization is 58.6 emu/gm. at 4.2°K (Daman, 1968).

CHAPTER V

DATA ANALYSIS

To analyze the data above 4.2°K a computer program was used which converted the thermocouple and magnetometer voltages to absolute units. A fixed thermocouple table was incorporated in the program's data. Corrections to this table were made at 4.2 and 77°K to agree with measured voltages at those temperatures. At all other temperatures a quadratic interpolation was used to adjust the table. This program sorted and averaged the susceptibility data within 1°K intervals.

Two experimental runs were made, one with the sample present and one without the sample, called the background. The background data was fitted by a least squares procedure to an expression of the form

$$Z(T) = \frac{C_b}{T} + Z_b$$

The sample a.c. susceptibility below 4.2°K is plotted as a function of temperature and compared with a plot of the results above 4.2°K.

RESULTS

The magnetic susceptibility of powdered $SmPO_4$ as a function of temperature is shown in Fig. 6 for $T > 4.2°K$. To a first approximation the data is expected to fall on a curve of the form $\chi = C/T + \chi_V$ where χ_V is the VanVleck term

Figure 6

Experimental and calculated susceptibility of $SmPO_4$ above 4.2°K. The calculated curve was obtained using K = 16 cm^{-1} and Δ = 1400 cm^{-1}. The points plotted are only a small fraction of the data collected and are intended to show the amount of scatter in the measurements and the temperature dependence of the deviation between the experimental values and the expression.

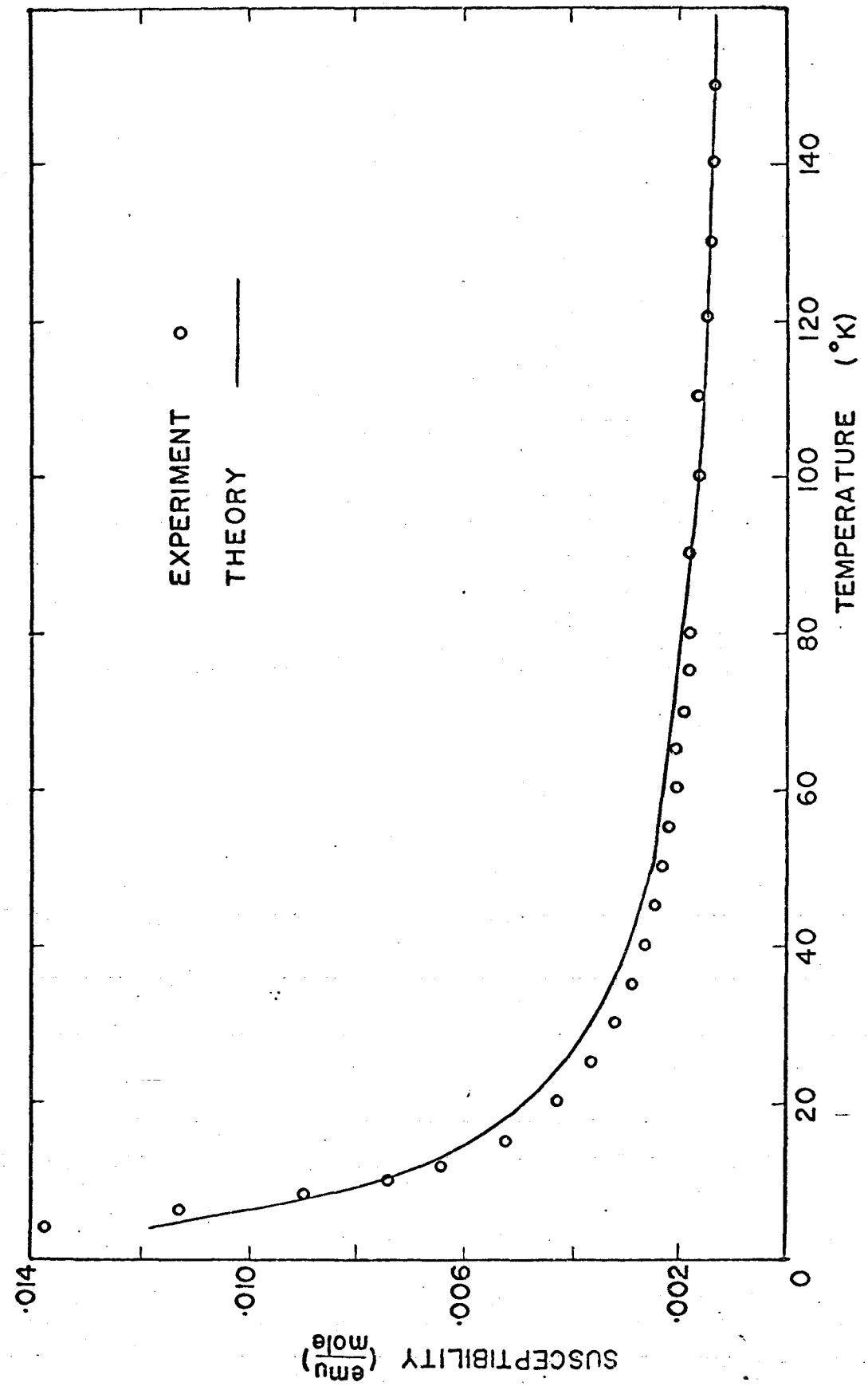
EXPERIMENT
THEORY
SUSCEPTIBILITY (emu/mole)
.014
.010
.006
.002
0
20
40
60
80
100
120
140
TEMPERATURE (°K)

Figure 6

and C is the Curie constant. The diamagnetic term is negligible as will be shown. A plot of χ versus 1/T (Fig. 7) gives a value of the VanVleck susceptibility, $\chi_V = (0.090 \pm .005) \times 10^{-2}$ emu/mole. A plot of $\chi-\chi_V$ versus 1/T indicates that the sample deviates from a Curie behaviour for T less than 10°K. Above this temperature, the curve was a straight line of slope $C_h = 6.1 \times 10^{-2}$ emu-°K/mole. Table 1 gives the measured and calculated susceptibility values for $SmPO_4$, over the temperature range from 4.2 to 180°K.

Results of the susceptibility for $T < 4.2$°K were preliminary. A graph of χ versus 1/T indicated that the data follows a Curie law over the range 4.2°K to 0.42°K with $C_\ell = 5.5 \times 10^{-2}$ emu-°K/mole. The results, however, are not consistent with the high temperature data.

The reason for the discrepancy may be magnetic impurities in the sample holder. More likely, however, is the uncertain state of the bridge calibration sample, CMN. It is believed that parts of this sample were in some unknown state of hydration and hence absolute values of the susceptibility could not be assigned. With this qualification, we present the low temperature results in Fig. 8.

Figure 7

A graph of the magnetic susceptibility of $SmPO_4$ above 4.2°K versus inverse temperature. The dotted line is an extrapolation of the linear portion of the curve above 10°K.

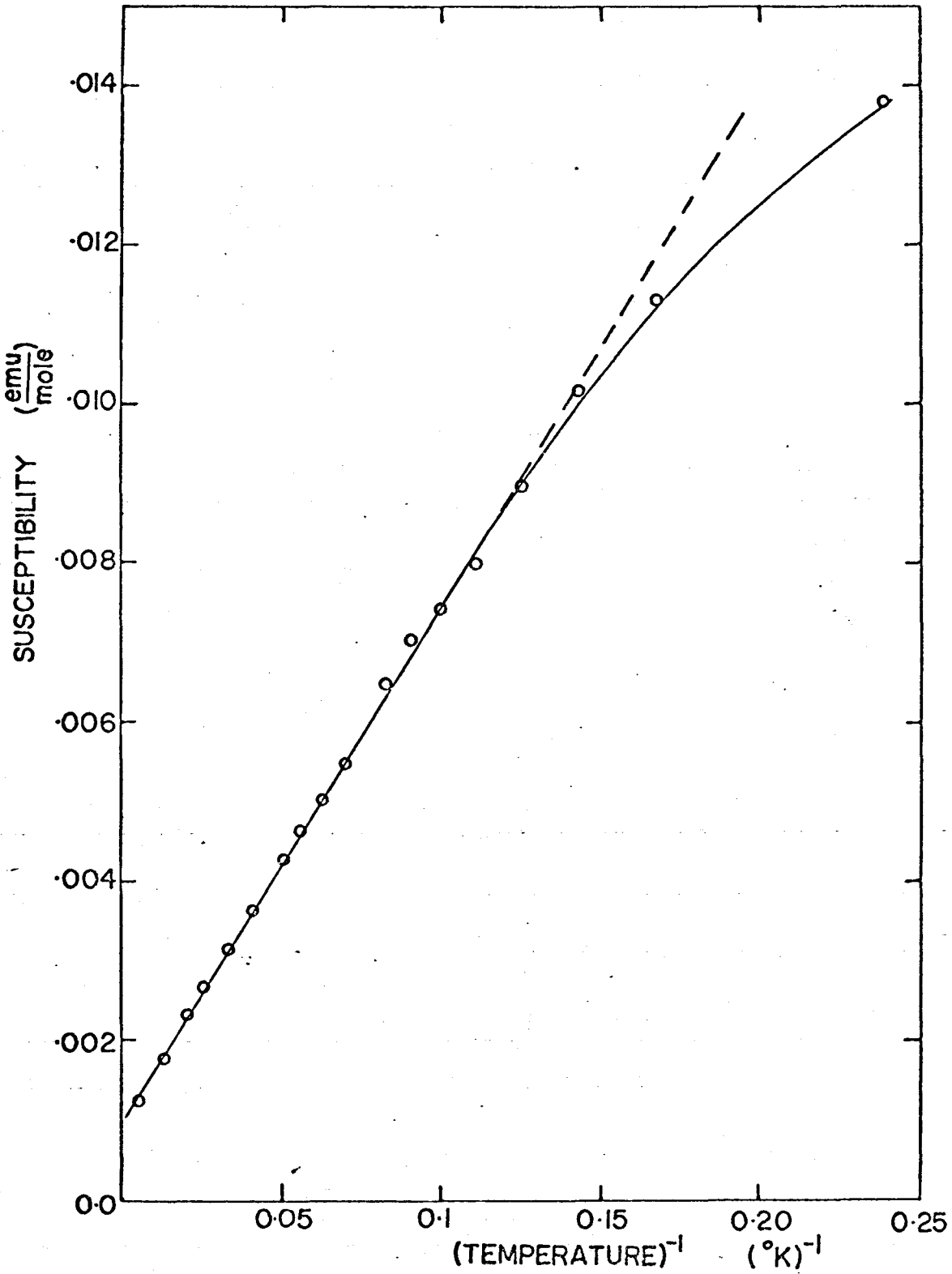
·014
·012
·010
·008
·006
·004
·002
0·0
SUSCEPTIBILITY (emu/mole)
0·05
0·1
0·15
0·20
0·25
(TEMPERATURE)⁻¹ (°K)⁻¹

Figure 7

Table 1

The experimental and calculated values of the susceptibility from 4.2°K to 180°K. T is the temperature (°K), χ_m is the measured susceptibility (emu/mole), χ_c is the calculated susceptibility (emu/mole) for K = 16 cm^{-1} and Δ = 1400 cm^{-1}. Values of χ_m above 180°K are not included due to a small signal-to-noise ratio above this temperature.

TABLE 1

MEASURED AND CALCULATED SUSCEPTIBILITY

OF POWDERED $SmPO_4$

T	$\chi_m x10^2$	$\chi_c x10^2$	T	$\chi_m x10^2$	$\chi_c x10^2$
4	1.38	1.18	5	-	1.07
6	1.13	.987	7	1.02	.923
8	.899	.867	9	.798	.817
10	.745	.772	11	.706	.731
12	.650	.693	13	.586	.658
14	.548	.627	15	.526	.598
16	.502	.572	17	.480	.548
18	.464	.526	19	.442	.505
20	.428	.487	21	.410	.470
22	.399	.454	23	.382	.439
24	.372	.425	25	.361	.412
26	.351	.400	27	.340	.389
28	.334	.379	29	.325	.369
30	.317	.360	31	.315	.351
32	.307	.343	33	.301	.336
34	.294	.328	35	.290	.321
36	.284	.315	37	.280	.309
38	.275	.303	39	.271	.297
40	.267	.292	41	.263	.287

Table 1 continued

T	$\chi_m x10^2$	$\chi_c x10^2$	T	$\chi_m x10^2$	$\chi_c x10^2$
42	.259	.282	43	.252	.277
44	.249	.273	45	.274	.269
46	.245	.264	47	.241	.261
48	.237	.257	49	.234	.254
50	.232	.250	51	.231	.247
52	.227	.244	53	.223	.240
54	.221	.237	55	.217	.235
56	.218	.232	57	.215	.229
58	.212	.227	59	.212	.224
60	.210	.222	61	.209	.219
62	.206	.217	63	.206	.215
64	.202	.213	65	.201	.211
66	.198	.209	67	.197	.207
68	.196	.205	69	.194	.203
70	.192	.201	71	.190	.200
72	.187	.198	73	.186	.196
74	.186	.195	75	.185	.193
76	.185	.192	77	.184	.190
78	.183	.189	79	.181	.187
80	.180	.186	81	.178	.185
82	.179	.183	83	.178	.182
84	.177	.181	85	.176	.180
86	.176	.178	87	.176	.177

Table 1 continued

T	$\chi_m x10^2$	$\chi_c x10^2$	T	$\chi_m x10^2$	$\chi_c x10^2$
88	.174	.176	87	.175	.175
90	.172	.173	91	.172	.173
92	.171	.172	93	.170	.171
94	.168	.170	95	.167	.169
96	.164	.168	97	.164	.167
98	.163	.166	99	.163	.165
100	.163	.164	102	.160	.163
104	.160	.161	106	.159	.159
108	.157	.158	110	.158	.156
112	.156	.155	114	.155	.154
116	.154	.152	118	.149	.151
120	.144	.150	122	.143	.149
124	.141	.147	126	.137	.146
128	.138	.145	130	.138	.144
132	.133	.143	134	.133	.142
136	.133	.141	138	.134	.140
140	.133	.139	142	.132	.138
144	.131	.137	146	.131	.137
148	.132	.136	150	.133	.135
152	.132	.135	154	.132	.134
156	.132	.133	158	-	.132
160	.130	.132	162	.131	.131
164	.129	.130	166	.129	.130
170	.127	.129	174	.127	.127
178	.127	.126	180	.126	.126

Figure 8

Preliminary results of the susceptibility measurements on $SmPO_4$ below 4.2°K. The points plotted are only a small fraction of the data collected and are intended to show the extent of the scatter in the measurements.

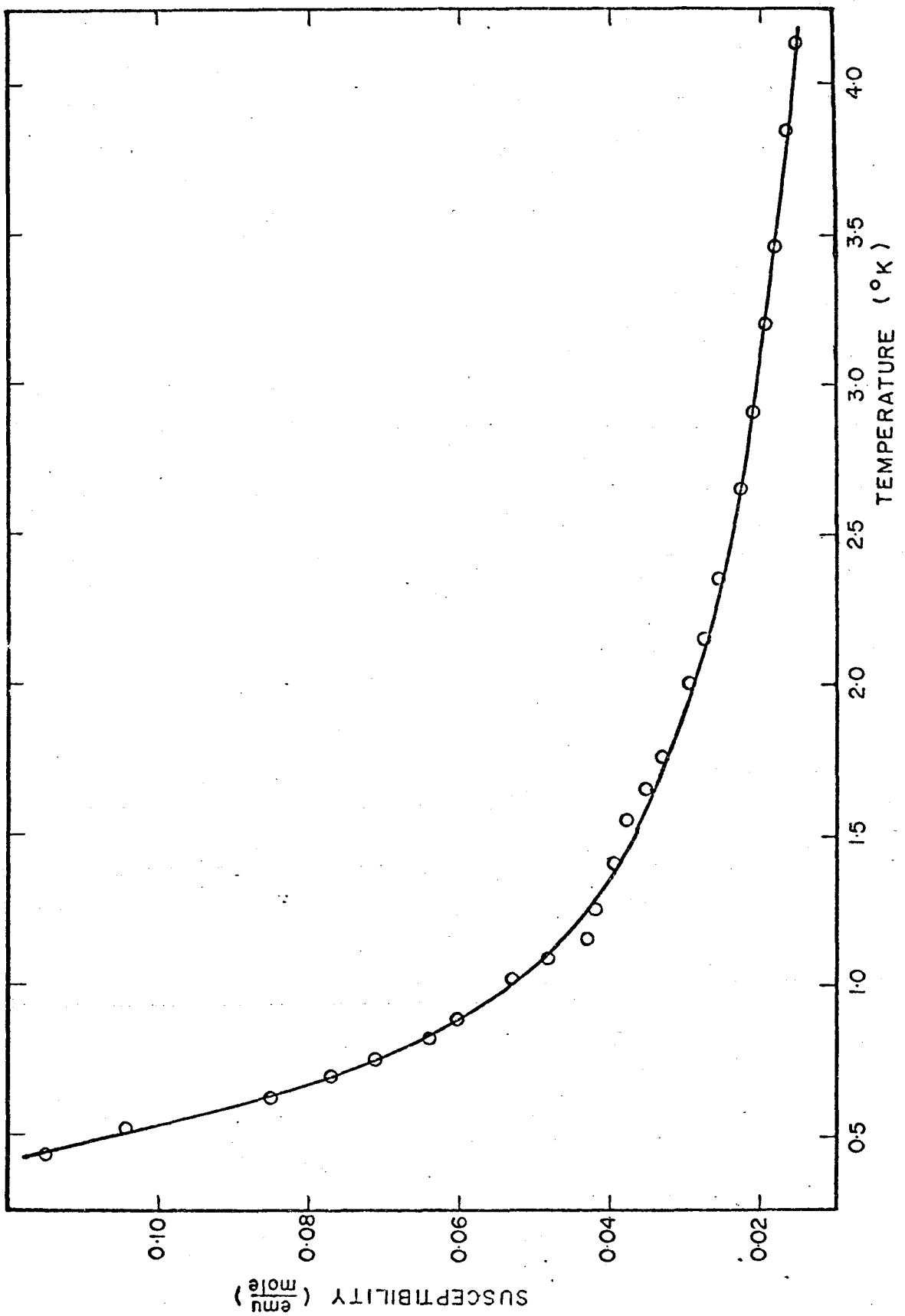
SUSCEPTIBILITY ($\frac{emu}{mole}$)
0·10
0·08
0·06
0·04
0·02
TEMPERATURE (°K)
0·5
1·0
1·5
2·0
2·5
3·0
3·5
4·0

Figure 8

CALCULATIONS

The secular matrix including the crystal and magnetic field effects is given in Fig. 9 where the unperturbed eigenfunctions are denoted by $|M\rangle$ and the quantum numbers J=5/2, L=5 and S=5/2 are common to all kets. The parameter 'a' is related to the crystal field parameter A_4^o by

$$a = A_4^o \, R/\sqrt{7}$$

where $R = (SLJ||Y_4||SLJ)$

and $d = \mu_o H/7$

The $\Gamma_7 - \Gamma_8$ splitting in terms of the above constants is

$$K = \frac{6}{\sqrt{7}} A_4^o \, R$$

The diagonalization of the matrix produced six eigenvalues in terms of the parameter K from which the values of μ_{nm} in the susceptibility expression could be calculated.

Values of K ranging from 0 to 150 $cm.^{-1}$ and of Δ ranging from 900 to 1500 $cm.^{-1}$ were substituted into the expression for χ to obtain a best fit to the measurements above 4.2°K. The values of K and Δ chosen are

$$K = 16 \pm 4 \text{ cm}^{-1}$$

$$\Delta = 1400 \pm 50 \text{ cm}^{-1}$$

Figure 9

The secular matrix for Sm^{3+} under a cubic crystalline and a magnetic field. Rows and columns are labelled by $|M\rangle$. The quantum number J = 5/2, L = 5 and S = 5/2 are common to all kets. The Parameter 'a' is proportional to 'K' and 'd' is proportional to the magnetic field H.

	$\|5/2\rangle$	$\|3/2\rangle$	$\|1/2\rangle$	$\|-1/2\rangle$	$\|-3/2\rangle$	$\|-5/2\rangle$
$\|5/2\rangle$	$a-5d$				$\sqrt{5}a$	
$\|3/2\rangle$		$-3a-3d$				$\sqrt{5}a$
$\|1/2\rangle$			$2a-d$			
$\|-1/2\rangle$				$2a+d$		
$\|-3/2\rangle$	$\sqrt{5}a$				$-3a+3d$	
$\|-5/2\rangle$		$\sqrt{5}a$				$a+5d$

Figure 9

Fig. 6 gives a comparison of the experimental and calculated susceptibility. The calculated curve is obtained by using the above value of K and Δ.

The perturbed energies and wavefunctions of the six levels of the $^6H_{5/2}$ ground state after application of a cubic crystal and a magnetic field are tabulated in Table 2.

Table 2

The calculated energies and wavefunctions of the $^6H_{5/2}$ ground state under a cubic crystal field and a magnetic field. The kets are of the form $|JM\rangle$

TABLE 2

Calculated energies and wavefunctions of the $^6H_{5/2}$ ground state under a cubic crystal field and a magnetic field using K = 16 cm^{-1} and and Δ= 1400cm^{-1}

ENERGY (cm^{-1})	WAVEFUNCTION
E_1 = 5.03	ψ_1 = 0.906 |5/2 5/2> + 0.423 |5/2-3/2>
E_2 = -10.5	ψ_2 = 0.423 |5/2 5/2> - 0.906 |5/2-3/2>
E_3 = 5.21	ψ_3 = |5/2 1/2>
E_4 = 5.32	ψ_4 = |5/2-1/2>
E_5 = 5.63	ψ_5 = 0.394 |5/2 3/2> + 0.919 |5/2-5/2>
E_6 = -10.8	ψ_6 = 0.919 |5/2 3/2> - 0.394 |5/2-5/2>

CHAPTER VI

DISCUSSION

This section contains a discussion of the errors involved in the measurements. An explanation of how the values of K and Δ were determined is given and the reliability of these values is discussed.

Since the sample susceptibility is large, the experimental errors in the high temperature measurements are approximately 2%. This was determined from past experience with other magnetic compounds. The background due to the sample holder is quite small so an error of 20% existed in the parameters C_b and Z_b. Since the background contribution to the susceptibility is less than 10% of the sample susceptibility, the background introduces only a 2% contribution to the error in the final result. The resultant error is then 4% in the sample susceptibility.

The low temperature results are preliminary. It is not possible to assign an error to these measurements. The rest of this discussion will pertain to the results above 4.2°K.

The temperature independent terms, namely, the VanVleck paramagnetism and the diamagnetism of the PO_4^{3-} and Sm^{3+} ions are not experimentally separable. The diamagnetic susceptibility of the PO_4^{3-} ion is tabulated as approximately 4×10^{-5} emu/mole (Foëx, 1957). It is expected that the diamagnetic susceptibility of the Sm^{3+} ion is less than this. The VanVleck term for

$SmPO_4$ is 9×10^{-3} emu/mole. Since the diamagnetic effects are negligible the experimental susceptibility quoted is that due to the 4f electrons on the Sm^{3+} ion.

The plot of χ versus 1/T (Fig. 7) indicates that the data follows a Curie law for temperatures greater than 10°K Below 10°K the susceptibility is lower than would be predicted by a Curie law extrapolation of the data above 4.2°K. This indicates that the assumption that the Γ_7 state lies lower in energy than the Γ_8 state is correct. This can be understood from the following argument.

The temperature dependence of the susceptibility can be written as a sum of two contributions in our case

$$\chi_T = (C(1) + e^{-K/kT} C(2))/T$$

where C(1) is the Curie constant of the ground state, either Γ_7 or Γ_8, and C(2) is the Curie constant of the remaining state. The Curie constant for a level is proportional to the square of the g-factor. Calculations of the g-factors for the Γ_7 and Γ_8 states indicate that $C(\Gamma_8)$ is greater than $C(\Gamma_7)$. Fig. 10 is a plot of χ_T versus 1/T. The graph shows schematically what one expects for the susceptibility if the Γ_7 state is lowest in energy and if the Γ_8 state is lowest in energy. A comparison of the curves in Fig. 10 with the experimental curve in Fig. 7 indicates that the Γ_7 state lies lowest.

Fig. 7 shows the extrapolation of the linear portion of the χ versus 1/T plot. The departure of our data from the

Figure 10

The temperature dependent part of the susceptibility is plotted in arbitrary units against inverse temperature. The solid curve represents the behaviour of the susceptibility if the Γ_7 state is assumed to lie lower in energy than the Γ_8 state and the dotted curve represents the behaviour if the Γ_7 and Γ_8 levels are inverted. The two curves are expected to depart from one another at a temperature T such that kT is approximately equal to K.

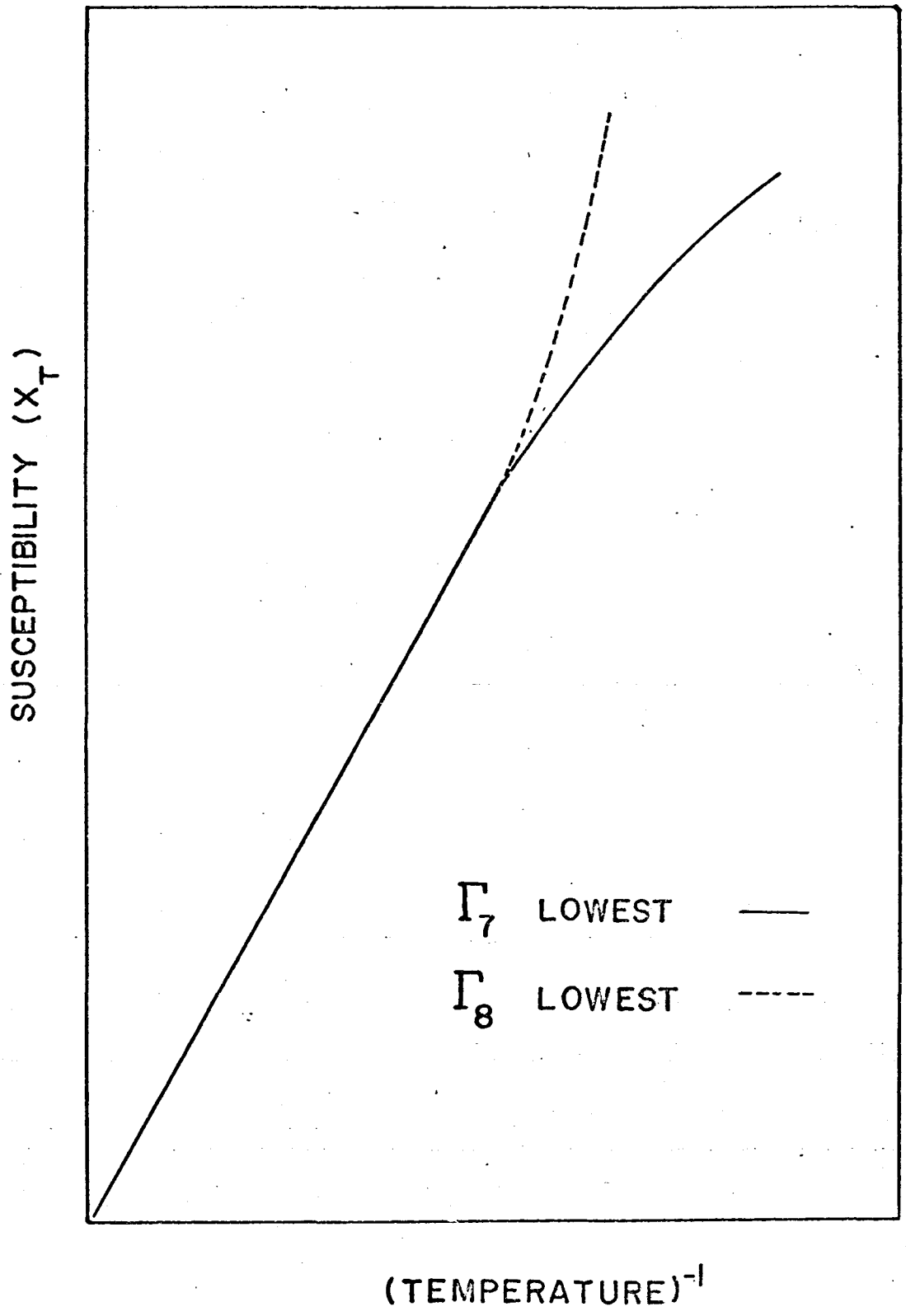
SUSCEPTIBILITY (X_T)
Γ_7 LOWEST
Γ_8 LOWEST
(TEMPERATURE)$^{-1}$

Figure 10

extrapolated curve is expected to occur at a temperature such that kT is of the order of K. This departure occurs at 10°K which suggests a value of K in reasonable agreement with our fitted value, 16 cm^{-1}.

We do not expect precise agreement of theory with experiment because of the assumption that the crystal field has cubic symmetry about the samarium ion. If we had included lower symmetry elements in the crystal field perturbation, we would have had enough parameters to generate any reasonable curve. Since no constraints are provided on the crystal field parameters by known energy splittings of the samarium ion levels, the cautious assumption of a cubic field seems appropriate.

For the best values of K and Δ the calculated values depart from the experimental values by 15% at most.

The choice of a suitable value of K was somewhat arbitrary. Fig. 11 is a plot of the calculated values of χ versus T for K = 10 and 20 cm^{-1}. The value of Δ was 1400 cm^{-1} in each case. The calculated results with K = 16 cm^{-1} lie between these curves.

CONCLUSIONS

The magnetic susceptibility of $SmPO_4$ follows a Curie law, after subtraction of a large temperature independent term, from room temperature down to about 10°K. The deviation from a Curie law below 10°K indicates that the overall crystal field splitting of the $^6H_{5/2}$ level of the Sm^{3+} ion is of the

Figure 11

The calculated susceptibility of $SmPO_4$ is plotted as a function of temperature for two cases: (i) $K = 10\ cm^{-1}$ and $\Delta = 1400\ cm^{-1}$ (ii) $K = 20\ cm^{-1}$ and $\Delta = 1400\ cm^{-1}$.

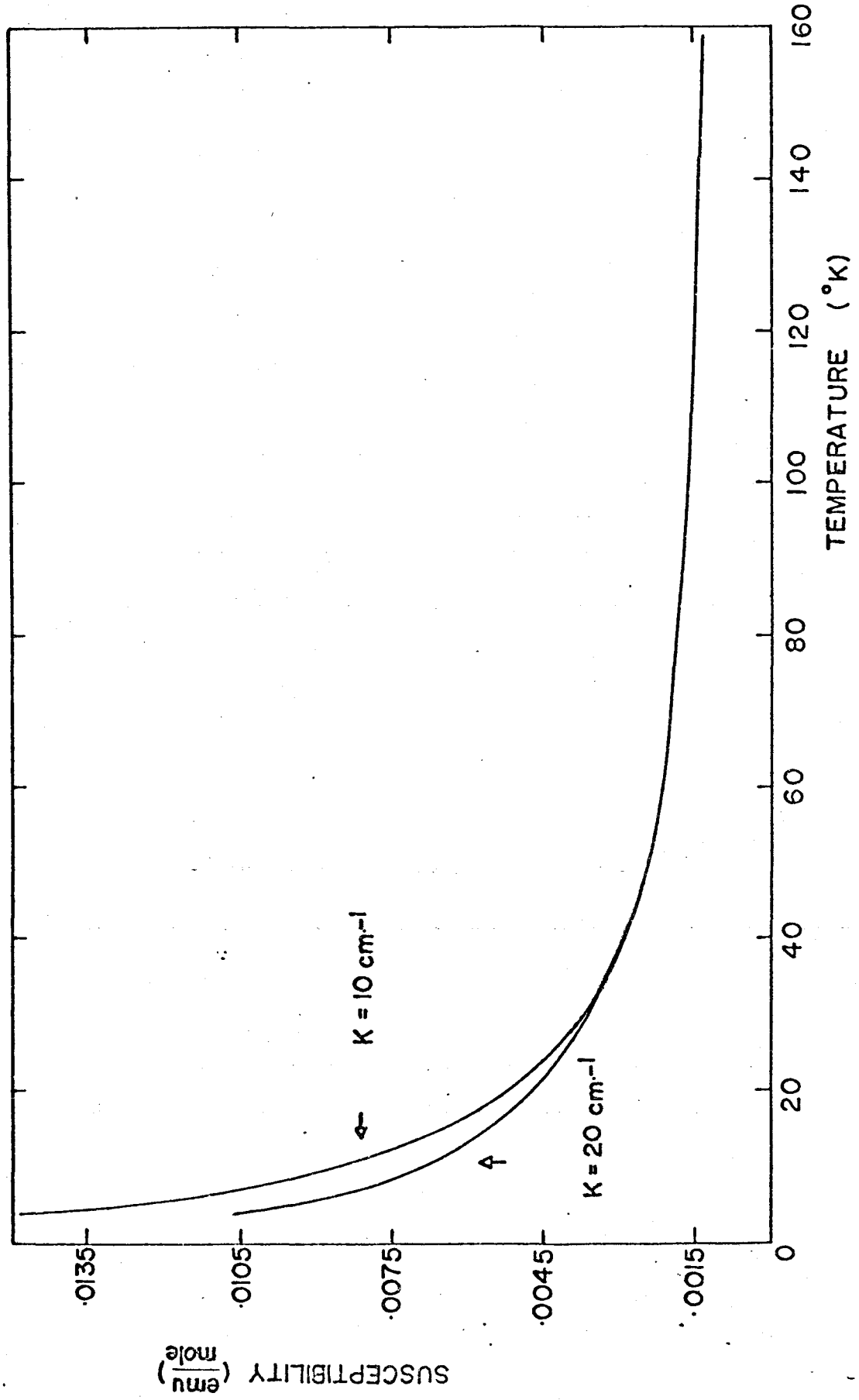
SUSCEPTIBILITY (emu/mole)
·0135
·0105
·0075
·0045
·0015
0
20
40
60
80
100
120
140
160
TEMPERATURE (°K)
K = 10 cm.⁻¹
K = 20 cm.⁻¹

Figure 11

order of 16 cm^{-1}. No magnetic ordering occurs in $SmPO_4$ down to 4.2°K. Although the results of the susceptibility measurements below 4.2°K are tentative, they indicate that no magnetic ordering occurs down to 0.4°K.

BIBLIOGRAPHY

1. Daman, H. et al. 1968 J. Appl. Phys. 39, 669.

2. Dieke, G.H. Spectra and Energy Levels of Rare Earth Ions in Crystals, Interscience Publishers, New York, 1968.

3. Feigelson, R.S., 1964. J. Am. Ceramic Soc. 47, 257.

4. Foëx, G., Constantes Sélectionnées Diamagnétisme et Paramagnétisme, Masson, 1957

5. Griffith, J.S., The Theory of Transition-Metal Ions, Cambridge University Press, 1964.

6. Low, W., Paramagnetic Resonance in Solids, Academic Press, New York and London, 1960.

7. Messiah, A., Quantum Mechanics II, Wiley New York, 1966.

8. Pillinger, W.L., P.S. Jastram and J.G. Daunt, 1958. Rev. of Sci. Instr. 29, 159.

9. Schriempe, J.T. and S.A. Friedberg, 1964. J. of Chem. Phys. 40, 296.

10. Schwarz, H., 1963. Z. Anorg. Allgem. Chem. 323, 44.

11. VanVleck, J.H., Electric and Magnetic Susceptibilities, Oxford University Press, New York, 1932.